Advanced Blanking Nonlinearity for Mitigating Impulsive Interference in OFDM Systems

Ulrich Epple and Michael Schnell, *Senior Member, IEEE*

***Abstract*—In this paper, we introduce advancements of the conventional blanking nonlinearity (BN) for orthogonal frequency-division multiplexing (OFDM)-based systems, which is referred to in the following as advanced BN. Blanking is a common measure for mitigating impulsive interference that often occurs in wireless communication systems. Although the BN removes impulsive interference reliably, it possesses various drawbacks for OFDM-based systems. In particular, the choice of the blanking threshold (BT), to decide whether a received sample is blanked, is a critical issue. We present an algorithm for determining the optimal BT to maximize the signal-to-noise-and-interference ratio (SINR) after blanking. Another drawback is that the entire received signal is discarded during a blanking interval, despite the fact that only a fraction of the spectrum of the OFDM signal might be affected by interference. We show how blanking can be limited to subcarriers that are actually affected by interference. Further, we show how these measures can be combined and how *a priori* information obtained in an iterative loop can be incorporated into the proposed scheme. Simulation results incorporating realistic channel and interference models demonstrate the effectiveness of the proposed scheme.**

***Index Terms*—Blanking nonlinearity (BN), impulsive interference, interference mitigation, orthogonal frequency division multiplexing (OFDM).**

I. Introduction

NOWADAYS, the multicarrier modulation technique orthogonal frequency-division multiplexing (OFDM) is deployed in numerous communication systems from a variety of different fields of applications. Consequently, OFDM signals may be exposed to various distortions, noise, and interference. The characteristics of these impairments highly depend on the transmission environment in which the respective OFDM system is deployed. For example, the distortions of an asymmetric digital subscriber line signal transmitted over wire differ significantly from the distortions of Wi-Fi signals in a home environment or from Long-Term Evolution (LTE) signals in a rural scenario. In addition, the receiver might be stationary in case of a digital video broadcast terrestrial (DVB-T) receiver at home or highly mobile for a mobile phone used in a car or in a train, leading to completely different distorting effects. In addition to distortions, in most applications, the OFDM signals are exposed to interference. The characteristics of the interference may also vary from system to system. The range of potential interference influences on to OFDM signals is clarified by the following examples. For power-line communications, the SNR is usually high, but impulsive interference, for example, generated by electrical devices connected to the power lines, has a significant influence. Wireless DVB-T signals may be impaired by impulsive interference, which is caused by house appliances. In urban environments, ignition systems generate impulsive interference on to LTE signals. In aeronautical communications, in the future, L-band digital aeronautical communications system type 1 (LDACS1) will be exposed to impulsive interference from distance measuring equipment (DME). In general, all wireless systems are susceptible to interference caused by other systems operating in the same frequency range. This interference impact is expected to increase over time with the implementation of new systems in conjunction with the scarcity of unused spectrum.

In many OFDM applications, the interference influence is small and well compensated by the spreading effect of the fast Fourier transform (FFT) in conjunction with channel coding. However, in case of strong interference or many different interference sources, the transmission performance of the OFDM system will degrade considerably if no countermeasures are taken. This issue puts the mitigation of interference in the focus of this investigation. In particular, we focus on the mitigation of impulsive interference since, in many applications, the interference occurs as short impulses.

Recently, there has been a lot of research on the mitigation of impulsive interference. A common approach for mitigating the impact of impulsive interference is to apply a memoryless blanking nonlinearity (BN) at the receiver input prior to the conventional OFDM demodulator [1], [2]. Iterative receiver structures for improving the performance of the BN are presented in [3] and [4]. It has also been suggested that the received signal is clipped at a certain level or that a combined blanking–clipping nonlinearity is applied [5], [6]. Decision-directed mitigation techniques are proposed in [7] and [8]. Recently, compressed-sensing-based mitigation algorithms have been suggested [9]–[11]. In [12] and [13], impulsive interference is mitigated based on appropriate coding and iterative decoding. An approach for exploiting the known spectral shape of impulsive interference is presented in [14].

In this paper, we elaborate on BN. Therefore, a blanking threshold (BT) is defined. Received signal parts with a

Manuscript received August 26, 2015; revised January 4, 2016; accepted February 15, 2016. Date of publication February 26, 2016; date of current version January 13, 2017. The review of this paper was coordinated by Dr. N.-D. Đào.

U. Epple was with the Institute of Communications and Navigation, German Aerospace Center (DLR), 82230 Oberpfaffenhofen, Germany (e-mail: epple.ulrich@gmail.com).

M. Schnell is with the Institute of Communications and Navigation, German Aerospace Center (DLR), 82230 Oberpfaffenhofen, Germany (e-mail: Michael.schnell@dlr.de).

Color versions of one or more of the figures in this paper are available online at http://ieeexplore.ieee.org.

Digital Object Identifier 10.1109/TVT.2016.2535374

magnitude exceeding BT are considered interference and are subsequently blanked. Although some of the other approaches mentioned earlier are more sophisticated and may lead to better performance under certain conditions, BN has some advantageous features that put it in the focus of this investigation. The main benefits of applying BN are the following.

- The BN offers a good tradeoff between computational complexity and achievable performance. Compared with most of the algorithms mentioned, the BN has much lower computational complexity. Consequently, it can be applied to a receiver without putting high requirements on the computational power.
- The BN does not rely on any information about the interference characteristics. That feature makes the BN robust against varying interference conditions during a transmission. Further, the BN removes any kind of impulsive interference, making it applicable to a wide range of systems.
- Since the BN is a blind approach, no possibly inaccurate estimation of interference parameters can degrade its performance. That makes the BN inherently robust and leads to a reliable mitigation of the impulsive interference.

Apparently, this list is only half the story. There also exist drawbacks of the BN in particular if applied in OFDM systems. They are summarized in the following.

- The determination of the BT is a sensitive task. The high peak-to-average power ratio (PAPR) of OFDM signals makes differentiation of interference pulses from OFDM signal peaks a challenging task. Correspondingly, a poorly chosen BT may impair the OFDM signal significantly.
- Another disadvantage of the BN is that the entire received signal is discarded during a blanking interval despite the fact that only a fraction of the spectrum of the OFDM signal might be affected by interference. In many cases, this feature leads to a waste of useful OFDM signal energy.
- The blanking of the OFDM signal by the BN introduces intercarrier interference (ICI) between the different subcarriers in the frequency domain. This effect limits the performance of the BN.

Currently, several algorithms to relieve these drawbacks of the BN have been published. In [15], an algorithm for determining the optimal BT to maximize the signal-to-interference-plus-noise ratio (SINR) is presented. In [16], it is shown how the waste of OFDM signal power in case of impulsive interference that affects the OFDM spectrum only partially can be minimized. Algorithms for mitigation ICI induced by the BN are presented in [3], [4], [17], and [18]. Applying these algorithms separately improves the performance of the transmission. However, the possibly achievable gain is limited.

In this paper, we present an OFDM receiver concept, termed advanced BN. This concept includes further developments of the algorithms from [15] and [16]. In addition, we show how these algorithms can be combined beneficially. In such a way, both the time and frequency domain characteristics of the impulsive interference are analyzed and subsequently exploited. Consequently, the gain by the advanced BN is significantly increased.

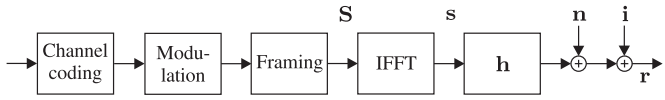

Fig. 1. Block diagram of OFDM transmission, including transmitter block, channel model, and impulsive interference.

II. System Model

Let us consider a digital baseband model of the transmission system. A stream of information bits enters an OFDM transmitter. The latter incorporates channel coding of the source bits, mapping of the coded bits on to modulated symbols, and insertion of pilot symbols. N modulated symbols S_k, $k = 0, 1, \ldots, N-1$, are arranged in a vector $\mathbf{S} = [S_0, S_1, \ldots, S_{N-1}]^T$ to form an OFDM symbol.[1] The vector $\mathbf{S}$ is then transformed into the time domain using an N-point inverse FFT (IFFT) to obtain the transmit vector $\mathbf{s} = [s_0, s_1, \ldots, s_{N-1}]^T$. In a real transmission, each OFDM symbol is preceded by N_{cp} cyclic prefix (CP) samples. Since we assume that the duration of the CP exceeds the channel impulse response (CIR) duration and a perfect time synchronization, the CP can be omitted in the model. The transmitted vector $\mathbf{s}$ is then used as input to a multipath channel with an impulse response $\mathbf{h} = [h_0, h_1, \ldots, h_{N-1}]^T$. It is assumed that $\mathbf{h}$ is constant at least for an OFDM symbol duration and that $h_l = 0$ for $l \geq N_{\mathrm{cp}}$, where l denotes the sample index in the time domain. We further assume that the received signal is corrupted by additive white Gaussian noise (AWGN) $\mathbf{n} = [n_0, n_1, \ldots, n_{N-1}]^T$ and impulsive interference $\mathbf{i} = [i_0, i_1, \ldots, i_{N-1}]^T$. Finally, the baseband model of the received signal can be represented as

$$\mathbf{r} = \mathbf{h} \circledast \mathbf{s} + \mathbf{n} + \mathbf{i} \tag{1}$$

where $\circledast$ denotes a circular convolution, and $\mathbf{r} = [r_0, r_1, \ldots, r_{N-1}]^T$ is a vector of received samples. The circular convolution is a direct consequence of omitting CP. Note that, for (1), a perfect frequency synchronization at the receiver is assumed. The signals $\mathbf{s}$, $\mathbf{n}$, and $\mathbf{i}$ can be assumed as statistically independent; further, without loss of generality, we assume that the power of the transmitted signal is normalized to one, i.e., $P_s = \mathbf{E}\{|s_l|^2\} = 2\sigma_s^2 = 1$. For the average power of the AWGN samples, it holds that $N_0 = 2\sigma_n^2$, with σ_s^2 and σ_n^2 being the componentwise variances of the transmit signal and the noise signal, respectively. The system model of the OFDM transmitter and the transmission channel as described earlier is summarized in Fig. 1.

The received signal $\mathbf{r}$ is passed to the OFDM demodulator. Similar to the OFDM modulation, the OFDM demodulation of $\mathbf{r}$ can be efficiently implemented by means of an FFT. Then, the output of the OFDM demodulator is denoted by $\mathbf{R} = [R_0, R_1, \ldots, R_{N-1}]^T$. When the OFDM subcarrier spacing is chosen such that ICI is avoided, R_k can be written as

$$R_k = H_k S_k + N_k + I_k \tag{2}$$

[1] Since the presented algorithm depends on information from the current received OFDM symbol only, the OFDM symbol index is omitted.

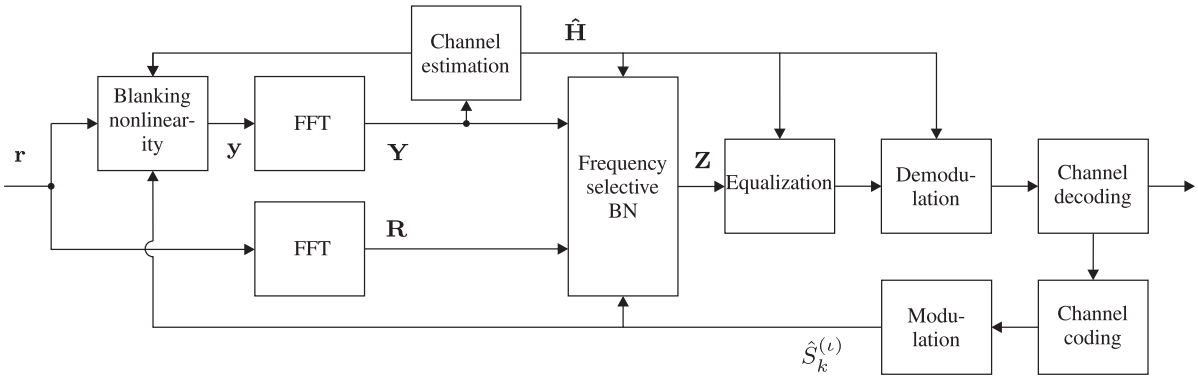

Fig. 2. Block diagram of iterative OFDM receiver including proposed interference mitigation.

with H_k being the kth sample of the channel transfer function (CTF) vector $\mathbf{H} = [H_0, H_1, \ldots, H_{N-1}]^T$. The CTF is the frequency-domain representation of the transmission channel, i.e., the FFT of the CIR $\mathbf{h}$. Accordingly, N_k and I_k are the kth samples of the vectors $\mathbf{N}$ and $\mathbf{I}$. They are obtained by a Fourier transform of the vectors $\mathbf{n}$ and $\mathbf{i}$.

To mitigate impulsive interference, we consider applying BN to the received signal $\mathbf{r}$ prior to the OFDM demodulation. Each received sample r_l with a magnitude exceeding a certain BT T^{BN} is set to zero. Mathematically, this can be described using a memoryless nonlinear mapping $f : \mathbb{C} \to \mathbb{C}$ specified as

$$y_l = f(r_l) = \begin{cases} r_l, & \text{if } |r_l| < T^{\mathrm{BN}} \\ 0, & \text{else} \end{cases} \tag{3}$$

for $l = 0, 1, \ldots, N-1$. The samples y_l for $l = 0, 1, \ldots, N-1$ form the vector $\mathbf{y}$, and after OFDM demodulation, one obtains the vector $\mathbf{Y} = [Y_0, Y_1, \ldots, Y_{N-1}]^T$. Obviously, such mitigation removes not only the interference but also the received OFDM signal and AWGN during the blanking intervals. To which extent the OFDM signal is impaired depends solely on the choice of BT. To remove as much interference as possible, BT should be as low as possible. However, a low threshold leads to significant impairment of the OFDM signal. Hence, the choice of BT is always a tradeoff between removing interference and preserving OFDM signal. This issue is addressed in detail in Section III.

The vector $\mathbf{Y}$ is passed to the channel estimation (CE) block. Based on inserted pilot symbols at certain subcarrier positions in certain OFDM symbols, estimates of the CTF, which is denoted by $\hat{\mathbf{H}} = [\hat{H}_0, \hat{H}_1, \ldots, \hat{H}_{N-1}]^T$, are determined in the CE block.

Next, the received signal and the blanked signal in the frequency domain $\mathbf{R}$ and $\mathbf{Y}$, as well as the estimated CTF $\hat{\mathbf{H}}$ are passed to the frequency-selective BN (FSBN) block. FSBN accounts for impulsive interference that affects merely a fraction of the OFDM signal bandwidth. By combining both signals $\mathbf{Y}$ and $\mathbf{R}$ appropriately, resulting in the combined signal $\mathbf{Z} = [Z_0, Z_1, \ldots, Z_{N-1}]^T$, the loss of useful OFDM signal caused by BN is minimized. The FSBN algorithm is presented in Section IV.

The estimates of the CTF $\hat{\mathbf{H}}$ allow an equalization of $\mathbf{Z}$ and subsequent demodulation. Typically, the goal of the demodulation is to provide the channel decoder with reliability information about the coded bits, which are further referred to as soft information. Based on such soft information, the channel decoder can achieve a much better performance compared with hard-decision coded bits, which are further referred to as hard information. Typically, log-likelihood ratios (LLRs) are deployed as soft information. Finally, the LLRs are passed to the channel decoding block, in which estimates of the transmitted uncoded bits are calculated. Note that depending on the applied channel coding scheme, one obtains either hard or soft information about the transmitted uncoded bits.

A well-known approach for improving the performance of an OFDM receiver is to apply an iterative receiver structure with iteration index ι. Such an approach often nearly achieves the performance of a maximum likelihood receiver. However, its computational complexity is significantly lower. In case of an iterative receiver structure, *a priori* information about the modulated symbols at each subcarrier k, which is denoted by $\hat{S}_k^{(\iota)}$, has to be determined based on the decoded bits. The calculation of $\hat{S}_k^{(\iota)}$ depends on the channel coding scheme. Some channel decoders directly calculate soft information about the coded bits, which can be subsequently soft modulated. In the case that the channel decoder calculated estimates of the uncoded bits, these bits have to be channel encoded and subsequently modulated. In this paper, we focus on the potentials of an iterative loop to improve the interference mitigation. Details are provided in Sections III and IV. The potentials of iterative loops for CE were assessed e.g., in [19] and [20]. Further potentials of iterative loops for the demodulation were evaluated, e.g., in [21] and [22].

The system model of the OFDM receiver structure, as described earlier, is clarified in Fig. 2.

III. Adaptive Blanking Threshold

In the following, we show how an optimal BT for BN can be calculated. This approach is a further development of the algorithm that we presented in [15]. The algorithm estimates SINR after BN, depending on T^{BN}. By maximizing this SINR, i.e.,

identifying T^{BN} that provides the highest SINR, one obtains the optimal BT, i.e.,

$$T^{\mathrm{BN}}_{\mathrm{opt}} = \arg\left(\max\left(\mathrm{SINR}(T^{\mathrm{BN}})\right)\right), \quad T^{\mathrm{BN}} > 0. \tag{4}$$

The given optimization method depends on a reliable estimation of the subcarrier SINR after BN. For deriving an expression for $\mathrm{SINR}(T^{\mathrm{BN}})$, we will first introduce two parameters. Let us define the remaining impulse interference after BN at subcarrier k by I'_k. This interference is caused by received samples comprising impulsive interference, however with a magnitude below BT. Then, the first parameter is the average remaining impulsive interference power at a subcarrier after the BN, given by $P_{I'}(T^{\mathrm{BN}}) = \mathbf{E}\{|I'_k|^2\}$. Next, let us define the sum of OFDM signal and AWGN at subcarrier k by $X_k = S_k + N_k$. The sum of the remaining OFDM signal and the remaining AWGN at subcarrier k after BN is denoted by X'_k. Then, we introduce the second parameter, i.e.,

$$K(T^{\mathrm{BN}}) = \frac{\mathbf{E}\left\{|X'_k|^2\right\}}{\mathbf{E}\left\{|X_k|^2\right\}} \tag{5}$$

which can be considered the average attenuation of the power of the sum of OFDM signal and AWGN by BN. Given these two parameters, according to [23] and [15], the subcarrier SINR can be expressed by

$$\mathrm{SINR}(T^{\mathrm{BN}}) = \frac{K^2(T^{\mathrm{BN}})P_s}{K(T^{\mathrm{BN}})\left(1-K(T^{\mathrm{BN}})\right)P_s + K(T^{\mathrm{BN}})N_0}, \cdots \frac{1}{+P_{I'}(T^{\mathrm{BN}})}. \tag{6}$$

The numerator consists of the remaining useful OFDM signal after BN. The denominator comprises three terms: ICI induced by BN, remaining AWGN after BN, and the remaining impulsive interference. In what follows, we briefly summarize the algorithm as presented in [15]. Note that the approach from [15] does only account for AWGN. In addition, it is assumed that the impulsive interference has a constant power spectral density (PSD). In this paper, we show how these two limitations can be overcome. In addition, we show how *a priori* information, typically obtained in an iterative loop, can improve the performance of BN. Note that our proposed algorithm does not require any information regarding the impulsive interference. It exploits the structure of the received signal, the OFDM signal power P_s, and the AWGN power N_0 before BN. Both power values are known in general or can be estimated easily in an OFDM receiver (see, e.g., [24] for AWGN or [25] for time-varying fading channels).

Note further that the calculation of the SINR according to (6) is based on some assumptions, summarized in the following. After BN, the remaining AWGN and impulsive interference are still white, i.e., comprise a constant PSD since the remaining AWGN and impulsive interference samples are still uncorrelated. Note that this assumption holds for Gaussian interference models but not for frequency-selective interference models. Furthermore, the remaining AWGN and impulsive interference can be assumed Gaussian distributed in the frequency domain, even for small numbers of impulsive interference samples and independently of the considered interference model. This assumption is explained by the noise bucket effect in [26]. In [23], it is shown that the ICI in the frequency domain can be assumed Gaussian distributed. The expected value of the useful OFDM signal power after the BN is equal for all subcarriers since on average each remaining time sample after the BN comprises equal contributions from all subcarriers.

A. Original Algorithm

To calculate the SINR from (6), we have to estimate 1) the remaining interference power $P_{I'}(T^{\mathrm{BN}})$ and 2) the attenuation factor $K(T^{\mathrm{BN}})$, as presented in the following.

Calculation of Remaining Interference Power $P_{I'}$: For obtaining the remaining interference power $P_{I'}$, we will first calculate the expected value of the total remaining energy $E_{w/I}$ after BN, depending on T^{BN}.

The calculation of $E_{w/I}$ is based on the magnitude probability density function (pdf) of the received signal $\mathbf{R}$. This pdf is denoted by $g_r(a)$, with received signal magnitude a. Since, in general, the interference conditions and, therefore, $g_r(a)$ are not known at the receiver, we propose to approximate $g_r(a)$ by the actual magnitude distribution of the N considered samples of an OFDM symbol. Now, based on $g_r(a)$, the total remaining energy $E_{w/I}$ after the BN can be calculated by

$$E_{\mathrm{w/I}} = N \int_0^{T^{\mathrm{BN}}} a^2 g_r(a)\,da. \tag{7}$$

The total number of nonblanked samples $N_{\mathcal{NB}}$ within the considered OFDM symbol is obtained by

$$N_{\mathcal{NB}} = N \int_0^{T^{\mathrm{BN}}} g_r(a)\,da. \tag{8}$$

Next, we are interested in the total energy $E_{wo/I}$ of these $N_{\mathcal{NB}}$ samples without interference, i.e., the total remaining OFDM and AWGN signal energy after BN. The exact value for $E_{wo/I}$ cannot be calculated without any knowledge about the interference. However, it can be approximated based on the magnitude pdf of the sum of OFDM and AWGN signal if no interference has occurred. Since these two signals are independent of each other and both Gaussian distributed, the magnitude pdf of their sum can be described by the Rayleigh distribution, i.e.,

$$f_{sn}(a) = \frac{a}{\sigma^2_{sn}} e^{-\frac{a^2}{2\sigma^2_{sn}}}, \quad a \geq 0 \tag{9}$$

with the constant variance $\sigma^2_{sn} = \sigma^2_s + \sigma^2_n$. The expected value of the power $P_{wo/I}$ of a sample with magnitude below T^{BN} without interference is now obtained when dividing the total energy by the number of respective samples. This is computed as

$$P_{wo/I} = \frac{N\int_0^{T^{\mathrm{BN}}} a^2 f_{sn}(a)\,da}{N\int_0^{T^{\mathrm{BN}}} f_{sn}(a)\,da}. \tag{10}$$

Finally, to determine the total energy $E_{wo/I}$ of $N_{\mathcal{NB}}$ samples, we have to multiply the average power $P_{wo/I}$ with the number of samples $N_{\mathcal{NB}}$

$$E_{wo/I} = N_{\mathcal{NB}} \cdot P_{wo/I}. \tag{11}$$

As the impulsive interference spreads equally over all subcarriers, the expected value for the remaining interference power $P_{I'}$ at a subcarrier is then obtained by

$$P_{I'} = \frac{\left(E_{w/I} - E_{wo/I}\right)}{N}. \tag{12}$$

Calculation of Attenuation Factor K: Remember the definition of K from (5). Obviously, $\mathbf{E}\{|X_k|^2\}$ from the denominator in (5) is given by $(P_s + N_0)$. The total remaining OFDM signal and AWGN energy after the BN $E_{wo/I}$ has been calculated in (11). Since this total energy spreads equally over all subcarriers, $\mathbf{E}\{|X'_k|^2\}$ from the numerator in (5) is obtained by dividing $E_{wo/I}$ by the number of considered samples N. Thus, K is computed as

$$K = \frac{E_{wo/I}}{N(P_s + N_0)}. \tag{13}$$

Note that in [23], K is defined as the ratio between the number of nonblanked samples per OFDM symbol and the number of total samples per OFDM symbol N. This is only an approximation when assuming that the blanking of a sample only depends on the impulsive interference but not on the OFDM signal and AWGN.

Given the results (12) and (13), we are now able to calculate the SINR based on (6). The optimal BT $T^{\mathrm{BN}}_{\mathrm{opt}}$ is subsequently obtained by applying (4). The BN algorithm including adaptive BT calculation is further referred to as adaptive BN.

B. Realistic Channel Conditions

In the presence of channel distortions, the algorithm for an adaptive BT calculation from Section III-A cannot be applied directly since the received subcarrier signal power is no longer P_s but may vary from subcarrier to subcarrier. Furthermore, the magnitude of the OFDM signal in the time domain is not necessarily Rayleigh distributed with componentwise variance $\sigma_s^2 = P_s/2$, a prerequisite for (9). In the following, it is shown how the algorithm for an adaptive BT calculation is adjusted to channel distortions by two measures.

At first, consider the magnitude distribution of the OFDM signal after passing a time-varying transmission channel. As explained in Section II, it can be assumed that CIR is quasi-constant for an OFDM symbol duration. From this, it follows that the magnitude of the samples of an OFDM symbol are still Rayleigh distributed, however, with a variance depending on the average power P_H of the transmission channel during the considered OFDM symbol, which is given by

$$P_H = \frac{\sum_{k=0}^{N-1} |H_k|^2}{N}. \tag{14}$$

This factor leads to a Rayleigh distribution of the magnitude of the sum of received OFDM signal and AWGN with componentwise variance $\sigma^2_{Hsn} = P_H\sigma_s^2 + \sigma_n^2$. Second, consider the SINR calculation from (6). Since, for a frequency-selective transmission channel, H_k differs for varying k, each subcarrier has a different SINR. Thus, the useful signal power in the numerator of (6) has to be multiplied by $|H_k|^2$. In addition, the ICI term in the denominator has to be adapted. In [23], it was shown, that on average all other subcarriers contribute evenly to ICI at the kth subcarrier. Consequently, the ICI term has to be multiplied by

$$P_{(H\backslash k)} = \frac{\sum_{\substack{n=0 \\ n\neq k}}^{N-1} |H_n|^2}{N-1}. \tag{15}$$

Since the variables $P_{(H\backslash k)}$ and P_H differ only in the contribution from the kth subcarrier, the approximation $P_{(H\backslash k)} \approx P_H$ is adopted in the following. Given these considerations and taking (6) into account, subcarrier SINR can be calculated by

$$\mathrm{SINR}_k(T^{\mathrm{BN}}) = \frac{K^2(T^{\mathrm{BN}})|H_k|^2 P_s}{K(T^{\mathrm{BN}})\left(1 - K(T^{\mathrm{BN}})\right) P_H P_s}, \cdots \frac{1}{+K(T^{\mathrm{BN}})N_0 + P_{I'}(T^{\mathrm{BN}})}. \tag{16}$$

To obtain BT maximizing the overall SINR, we have to calculate the average $\mathrm{SINR}_{\mathrm{av}}$ of all subcarriers and maximize this term. Based on (16) and (14), $\mathrm{SINR}_{\mathrm{av}}$ is calculated by

$$\mathrm{SINR}_{\mathrm{av}}(T^{\mathrm{BN}}) = \frac{\sum_{k=0}^{N-1} \mathrm{SINR}_k(T^{\mathrm{BN}})}{N} \tag{17}$$

$$= \frac{K^2(T^{\mathrm{BN}})P_H P_s}{K(T^{\mathrm{BN}})\left(1 - K(T^{\mathrm{BN}})\right) P_H P_s}, \cdots \frac{1}{+K(T^{\mathrm{BN}})N_0 + P_{I'}(T^{\mathrm{BN}})}. \tag{18}$$

This result shows that the calculation of BT can be adjusted to realistic channel conditions by incorporating the average power P_H of CTF for the current OFDM symbol. Note that since, in general, BN is applied to the time-discrete received signal prior to other receiver components, no information regarding the transmission channel is available, and an AWGN channel has to be assumed. However, CTF is estimated by means of CE later on in the receiver. This estimate of CTF can be incorporated in the BN to improve BT calculation in an iterative loop, as described in Section III-D.

C. Frequency-Selective Interference

To calculate the remaining impulsive interference by (12), it is assumed that the impulsive interference spreads equally over all subcarriers. In reality, this assumption might not always be valid, and merely certain subcarriers might be affected by interference. In what follows, we show how the remaining

subcarrier impulsive interference $P_{I'}$ can be approximated for frequency-selective impulsive interference.

In general, no knowledge regarding the subcarrier interference signal is available at BN. Hence, the subcarrier interference power can only be approximated based on known statistics regarding the received signal without interference. Since a separate approximation for each subcarrier is not accurate, we propose to estimate the impulsive interference power jointly for a set of certain adjacent subcarriers, i.e., a so-called bin. The number of subcarriers per bin is always a tradeoff. For large bin sizes, the estimation error is getting less and less due to averaging, leading to more meaningful estimates of the subcarrier interference power. However, the frequency-selective behavior is not well reflected by large bin sizes. Therefore, we propose to split the N OFDM subcarriers into M bins,[2] each with $N_M = N/M$ subcarriers. The set of subcarrier indices of each bin $m = 0, 1, \ldots, M-1$ is given by $\mathcal{K}_m = \{mN_M, mN_M + 1, \ldots, (m+1)N_M - 1\}$. The number of bins M can be determined in a blind approach. In this case, a value of $M \approx \sqrt{N}$ seems to be a good tradeoff between remaining estimation error and reflecting the frequency-selective behavior. The determination of the optimal M would require information about interference and channel characteristics and is beyond the scope of this paper. However, it should be remarked that if M is selected according to known or estimated interference characteristics, the proposed advanced BN is no longer a blind approach.

Next, we calculate an average subcarrier impulsive interference power $P_{i,m}$ for each bin with index m. Consider the received subcarrier signal R_k. Given that no interference is present at the kth subcarrier, i.e., $I_k = 0$, the expected received power is given by

$$\mathbf{E}\left\{|R_k|^2 | I_k = 0\right\} = |H_k|^2 P_s + N_0. \tag{19}$$

Based on (19), an estimate for the average received impulsive interference power of the mth bin is calculated by

$$P_{i,m} = \frac{\sum\limits_{k \in \mathcal{K}_m} \left(|R_k|^2 - \mathbf{E}\left\{|R_k|^2 | I_k = 0\right\}\right)}{N_M}. \tag{20}$$

Since we are interested in the remaining impulsive interference after BN, the attenuation of the impulsive interference $P_{i,m}$ in dependence of BT has to be calculated next. Based on (7) and (11), the total remaining impulsive interference energy after BN is obtained by $E_{i'} = E_{w/I} - E_{wo/I}$. The total impulsive interference energy E_i before BN can be calculated by (7) for $T^{\mathrm{BN}} \to \infty$. Similar to (5), we can calculate a factor K_i, defining the instantaneous attenuation of the impulsive interference, i.e.,

$$K_i = \frac{E_{i'}}{E_i}. \tag{21}$$

[2]For simplicity, we restrict the choice of M to $N \mod M = 0$. In principle, each $M \leq N$ is possible. In this case, the number of subcarriers per bin is not constant.

When assuming that each spectral part is equally attenuated by BN, the average remaining impulsive interference power for each bin can be calculated by

$$P_{i',m} = K_i P_{i,m}. \tag{22}$$

Next, we define the average power of the transmission channel for the mth bin as

$$P_{H,m} = \frac{\sum\limits_{k \in \mathcal{K}_m} |H_k|^2}{N_M}. \tag{23}$$

Based on this result, we can adjust the calculation of the subcarrier SINR from (16) to frequency-selective interference and obtain the SINR estimate for the mth bin as

$$\mathrm{SINR}_m = \frac{K^2 P_{H,m} P_s}{K(1-K) P_H P_s + K N_0 + K_i P_{i,m}}. \tag{24}$$

To obtain BT maximizing SINR, we have to calculate the average $\mathrm{SINR}_{\mathrm{av}}$ of all bins according to (17) and maximize this term. In this way, the BT calculation is adapted to frequency-selective impulsive interference.

D. Potentials of Iterative Loop

It is well known that OFDM signals have a relatively high PAPR. This property makes differentiation of interference impulses from OFDM signal peaks challenging. Specifically, the high PAPR leads to a blanking of OFDM signal peaks if applying the BN according to (3). This issue can be relieved by taking *a priori* information into account. The idea is to apply a second metric in addition to the magnitude of the received signal to distinguish between impulsive interference and OFDM signal peaks. We calculate the estimated subcarrier interference by

$$\hat{I}_k^{(\iota)} = R_k - \hat{H}_k \hat{S}_k^{(\iota)} = I_k + N_k + N_{k,\mathrm{rem}}^{(\iota)}. \tag{25}$$

The term $N_{k,\mathrm{rem}}^{(\iota)}$ accounts for inaccurately estimated channel coefficients and imperfect *a priori* information. Consequently, when assuming perfect *a priori* and channel knowledge, (25) simplifies to

$$\hat{I}_k^{(\iota)} = I_k + N_k. \tag{26}$$

The corresponding signal in the time domain after IFFT writes

$$\hat{i}_l^{(\iota)} = i_l + n_l. \tag{27}$$

The signal $\hat{i}_l^{(\iota)}$ can be considered an estimate of the impulsive interference in the time domain disturbed by AWGN. This allows us to apply a hypothesis test to decide whether impulsive interference occurred or not. Assume that no interference is present and that perfect *a priori* information and channel knowledge is available. Then, $\hat{i}_l^{(\iota)}$ is obviously Gaussian distributed with componentwise variance σ_n^2. This allows us to formally pose the impulsive interference detection problem as a composite statistical hypothesis test as follows.

Define the hypotheses $\mathcal{H}_0 : i_l = 0$ and $\mathcal{H}_1 : i_l \neq 0$. Under $\mathcal{H}_0$, $|\hat{i}_l^{(\iota)}|$ follows a Rayleigh distribution with the scale parameter σ_n^2. Under $\mathcal{H}_1$, the situation is different since $|\hat{i}_l^{(\iota)}|$ now follows a distribution of the mixture of i_l and n_l. Thus, to decide between $\mathcal{H}_0$ and $\mathcal{H}_1$ in a Neyman–Pearson-like sense [27], we fix the probability of the type-I error at some level p_I. The type-I error is defined as the probability of selecting $\mathcal{H}_1$ when $\mathcal{H}_0$ is true. Then, the optimal hypothesis $\hat{\mathcal{H}}$ is selected as

$$\hat{\mathcal{H}} = \begin{cases} \mathcal{H}_0 : & \left|\hat{i}_l^{(\iota)}\right| < \mathcal{T}_i \\ \mathcal{H}_1 : & \left|\hat{i}_l^{(\iota)}\right| \geq \mathcal{T}_i \end{cases} \tag{28}$$

where the decision threshold $\mathcal{T}_i$ is calculated by

$$\mathcal{T}_i = \sqrt{\sigma_n^2 \log\left(\frac{1}{p_I}\right)}. \tag{29}$$

Equation (29) follows directly from the cumulative Rayleigh distribution function. Now, a received sample is only blanked if $\mathcal{H}_1$ is selected and if the received signal magnitude exceeds BT.

In addition to this hypothesis test, *a priori* information can also improve the calculation of the adaptive BT T^{BN}. Specifically, *a priori* information can be used to improve the estimation of the impulsive interference power in the frequency domain from (20). The idea is to calculate this power rather based on $\hat{I}_k^{(\iota)}$ than on R_k. Since the initially unknown OFDM signal is subtracted in (25), a more accurate estimate is expected. According to (19), we define

$$\mathbf{E}\left\{\left|\hat{I}_k^{(\iota)}\right|^2 | I_k = 0\right\} = N_0. \tag{30}$$

Now, it is straightforward to replace (20) by

$$P_{i,m} = \frac{\sum\limits_{k\in\mathcal{K}_m}\left(\left|\hat{I}_k^{(\iota)}\right|^2 - \mathbf{E}\left\{\left|\hat{I}_k^{(\iota)}\right|^2 | I_k = 0\right\}\right)}{N_M} \tag{31}$$

for $\iota > 0$. However, it should be emphasized that the accuracy of this approach strongly depends on $N_{k,\mathrm{rem}}^{(\iota)}$. Given imperfect *a priori* and channel knowledge, the contribution from $N_{k,\mathrm{rem}}^{(\iota)}$ will distort the estimation of the interference power, and the algorithm from (31) may even lead to a performance degradation.

IV. Frequency-Selective Blanking Nonlinearity

During the blanking interval, the entire OFDM signal is discarded, despite the fact that only a fraction of the OFDM spectrum might be affected by interference. To relieve this issue, we have introduced the FSBN scheme in [16]. The following considerations are based on this investigation. The proposed FSBN scheme profits from combining the received signal with the signal after the BN. The approach is realized by first detecting the interference at each subcarrier using a new Neyman–Pearson-like testing procedure [27]. Provided that interference has been detected, both the received and the blanked signal are subsequently optimally combined to maximize the SINR for each subcarrier. In this way, the proposed algorithm compensates losses due to falsely blanked OFDM signal samples that are not corrupted by interference. In addition, the blanking of the OFDM signal is restricted to subcarriers that are actually affected by impulsive interference.

At first, we briefly describe the FSBN algorithm assuming a fixed predefined BT, based on [16]. Then, it is shown how the BT calculation from Section III, originally derived for BN, has to be adjusted to FSBN, which was not addressed in [16]. Finally, we consider potential gains of FSBN in an iterative loop.

A. Principle

Consider the block diagram of the proposed OFDM receiver structure including FSBN, which is shown in Fig. 2. The block diagram illustrates that the FSBN is a joint time (BN block) and frequency (FSBN block) domain interference mitigation approach. Such a joint approach enables taking the spectral characteristics of the impulsive interference and its time domain structure into account.

The combined signal $\mathbf{Z}$ is computed to maximize the SINR for each subcarrier, as explained in the following. It should be noted that the algorithm does not rely on a known shape or model of the interference, neither in the time nor frequency domain. First, we need to detect and estimate the interference power at each subcarrier. Therefore, we assume that the impulsive interference I_k in the frequency domain is Gaussian distributed for an individual subcarrier k. In [26], it is shown that this approximation is valid independently of the structure of the impulsive interference due to the spreading effect of the FFT. According to [16] and [23], the signal Y_k after BN and FFT is represented as follows:

$$Y_k = KH_kS_k + D_k + N_k'. \tag{32}$$

The distortion term D_k accounts for the ICI induced by BN, and N_k' denotes AWGN after BN. Equations (2) and (32) allow us to define the FSBN indicator signal as follows:

$$\Delta Y_k = R_k - \frac{Y_k}{K} = I_k + \left(N_k - \frac{N_k'}{K}\right) - \frac{D_k}{K}. \tag{33}$$

Denoting the AWGN part of the FSBN indicator signal by

$$\Delta N_k = N_k - \frac{N_k'}{K} \tag{34}$$

and defining the FSBN distortion term as

$$D_k' = \Delta N_k - \frac{D_k}{K} \tag{35}$$

we can write the FSBN indicator signal from (33) as

$$\Delta Y_k = I_k + D_k'. \tag{36}$$

The signal ΔY_k is a useful indicator whether the kth subcarrier is affected by interference. Indeed, if $I_k = 0$, ΔY_k equals D_k' only; otherwise, ΔY_k will include the combination of D_k' and impulsive interference I_k. Unfortunately, the signal D_k' is not available at the receiver. However, we can approximate its

statistics. At first, we consider the AWGN term ΔN_k. This term describes a zero-mean Gaussian process. Its variance can be derived based on (34). After some calculations [16], the variance of ΔN_k is obtained by

$$\mathrm{Var}(\Delta N_k) = \frac{1-K}{K} N_0. \tag{37}$$

Second, we consider the distortion term D_k. In [23], it is shown that the distortion term D_k can be approximated by a zero-mean complex Gaussian process with variance $\mathrm{Var}(D_k) = K(1-K)P_H P_s$. Note that this term is basically the ICI term from (16). Since ΔN_k and D_k are statistically independent, the variance of D'_k can be approximated by

$$\mathrm{Var}\left(D'_k\right) = \frac{(1-K)}{K}(P_H P_s + N_0). \tag{38}$$

The result from (38) allows us to formally pose the impulsive interference detection problem as a composite statistical hypothesis test as follows.

Define the hypotheses $\mathcal{H}_0 : I_k = 0$ and $\mathcal{H}_1 : I_k \neq 0$, and consider the distribution of $|\Delta Y_k|$ under these hypotheses. Under $\mathcal{H}_0$, $|\Delta Y_k|$ follows a Rayleigh distribution with the scale parameter $\mathrm{Var}(D'_k)$. Under $\mathcal{H}_1$, the situation is different since $|\Delta Y_k|$ now follows a distribution of the mixture of D'_k and I_k. Assuming that for a specific k the interference I_k is Gaussian, we have the following. If I_k is zero mean, then $|\Delta Y_k|$ can be approximated with a Rayleigh distribution, yet with a larger scale parameter that accounts for the variance of I_k. When I_k is not zero mean, then $|\Delta Y_k|$ can be approximated with a Rician distribution. Thus, we need to decide between $\mathcal{H}_0$, when $|\Delta Y_k|$ follows a Rayleigh distribution, and a composite alternative $\mathcal{H}_1$, when $|\Delta Y_k|$ follows a Rician distribution or a Rayleigh distribution with a larger scale parameter. Note that this is a one-sided test. Moreover, the critical region of such a test is independent of the statistics of I_k but depends merely on the statistics of D'_k, which are known [27]. In other words, the critical region depends on the distribution of $|\Delta Y_k|$ under the hypothesis $\mathcal{H}_0$. To decide between $\mathcal{H}_0$ and $\mathcal{H}_1$ in a Neyman–Pearson-like sense, we fix the probability of the type-I error at some level p_I. A type-I error is defined as the probability of selecting $\mathcal{H}_1$ when $\mathcal{H}_0$ is true. Then, the optimal hypothesis $\hat{\mathcal{H}}$ is selected as

$$\hat{\mathcal{H}} = \begin{cases} \mathcal{H}_0 : & |\Delta Y_k| < \mathcal{T}_{\mathcal{H},k} \\ \mathcal{H}_1 : & |\Delta Y_k| \geq \mathcal{T}_{\mathcal{H},k} \end{cases} \tag{39}$$

where the decision threshold $\mathcal{T}_{\mathcal{H},k}$ is calculated by

$$\mathcal{T}_{\mathcal{H},k} = \sqrt{\mathrm{Var}\left(D'_k\right) \log\left(\frac{1}{p_I}\right)}. \tag{40}$$

Equation (40) follows directly from the cumulative Rayleigh distribution function. Obviously, if $\mathcal{H}_0$ is selected, then $Z_k = R_k$ as there is no impulsive interference. However, if $\mathcal{H}_1$ is selected, then R_k and Y_k have to be optimally combined based on their subcarrier SINR to obtain Z_k. Under the assumption that I_k and D'_k are uncorrelated, the interference power at the kth subcarrier can be computed from (36) and (38) as

$$|I_k|^2 = \begin{cases} |\Delta Y_k|^2 - \mathrm{Var}\left(D'_k\right), & \text{if } |\Delta Y_k| \geq \mathcal{T}_{\mathcal{H},k} \\ 0, & \text{else} \end{cases}. \tag{41}$$

Next, we consider an optimal combination of R_k and Y_k that maximizes the SINR. For that purpose, we calculate the combined subcarrier signal Z_k by

$$Z_k = w_k R_k + (1-w_k) Y_k \tag{42}$$

where $w_k \in [0,1]$ is a weighting factor. It is now straightforward to obtain the SINR of the combined signal Z_k as a function of the weighting factor w_k, i.e.,

$$\mathrm{SINR}_{Z_k} = \frac{|H_k|^2 P_s \left(w_k + (1-w_k)K\right)^2}{w_k^2 |I_k|^2 + (1-w_k)^2 K(1-K) P_H P_s}, \cdots \\ \frac{1}{+ \left(K + w_k^2(1-K)\right) N_0}. \tag{43}$$

After some algebra, the extremum of (43) with respect to w_k is found at

$$w_k = \begin{cases} \frac{(1-K)(P_H P_s + N_0)}{(1-K)(P_H P_s + N_0) + |I_k|^2}, & \mathcal{H}_1 \text{ is selected} \\ 1, & \mathcal{H}_0 \text{ is selected.} \end{cases} \tag{44}$$

Obviously, when no blanking is applied, i.e., $K = 1$ or no interference is detected ($I_k = 0$) for a specific k, the signal Y_k is discarded as it contains no additional information. In all other cases, both the received signal R_k and the blanked signal Y_k are linearly combined with the weighting factor chosen to maximize the SINR.

B. Adjustment of Blanking Threshold Calculation

When applying FSBN, the adaptive BT calculation from Section III has to be adjusted. Remember that BT is obtained by maximizing the SINR after BN. In (24), it is shown how the calculation of the BT T^{BN} is adjusted to frequency-selective interference. Now, when considering that the blanked signal is combined with the received signal, T^{BN} should rather be obtained to maximize SINR after the combination of both signal from (43). The SINR calculation from (43) requires knowledge of the subcarrier interference power $|I_k|^2$. However, such knowledge is not available at BN. In the following, it is shown how $|I_k|^2$ can be approximated and, subsequently, how an adaptive BT can be calculated for FSBN. In the following, the FSBN with adaptive BT calculation is referred to as adaptive FSBN.

Remember Section III-C, where the OFDM bandwidth is segmented into M bins. Given the approximation that the subcarrier impulsive interference power is constant within a bin, we can expect that $|I_k|^2 \approx P_{i,m}$ for $k \in \mathcal{K}_m$. When taking this

approximation and (24) into account, we are able to write an approximated version of (43) for each bin m

$$\mathrm{SINR}_m = \frac{P_{H,m}P_s\left(w_m+(1-w_m)K\right)^2}{\left(K_i+w_m^2(1-K_i)\right)P_{i,m}},\cdots,\\ \frac{1}{+(1-w_m)^2K(1-K)P_HP_s+\left(K+w_m^2(1-K)\right)N_0}. \tag{45}$$

The estimated SINR_m from (45) leads also to a different result for the weighting factor w_m, which is now constant for the bin with index m. Similar to (44), the weighting factor w_m can be obtained by

$$w_m = \frac{(1-K)K(P_HP_s+N_0)+(1-K)K_iP_{i,m}}{(1-K)K(P_HP_s+N_0)+K(1-K_i)P_{i,m}}. \tag{46}$$

Based on (45) and (46), we are now able to calculate the SINR_m for each bin. To obtain BT which maximizes SINR, we have to calculate the average $\mathrm{SINR}_{\mathrm{av}}$ of all bins according to (17) and maximize this term. In this way, the BT calculation is adjusted to FSBN.

C. A Priori Information for FSBN

If an iterative receiver structure is applied, the detection of subcarrier interference and the calculation of the interference power can also profit from *a priori* information. Consider the signal $\hat{I}_k^{(\iota)}$ from (26). This term is similar to D'_k from (35). If no impulsive interference occurs, both terms $\hat{I}_k^{(\iota)}$ and D'_k follow a Gaussian distribution with known variances $\mathrm{Var}(D'_k)$ for D'_k from (38) and N_0 for $\hat{I}_k^{(\iota)}$ from (26). This similarity allows application of the hypothesis test explained in Section IV-A to the signal $\hat{I}_k^{(\iota)}$ as well to obtain an additional estimate $|I_{\mathrm{iter},k}|^2$ of the impulsive interference power in accordance to (41) by

$$|I_{\mathrm{iter},k}|^2 = \begin{cases} \left|\hat{I}_k^{(\iota)}\right|^2 - N_0, & \text{if } \left|\hat{I}_k^{(\iota)}\right| \geq \mathcal{T}_{\mathcal{H},k} \\ 0, & \text{else.} \end{cases} \tag{47}$$

The decision threshold $\mathcal{T}_{\mathcal{H},k}$ can be calculated by (40), but with variance N_0. Since D'_k consists mainly of ICI and has only a small AWGN contribution, whereas $\hat{I}_k^{(\iota)}$ consists mainly of AWGN, both estimates of the impulsive interference power $\left|\hat{I}_k^{(\iota)}\right|^2$ and $|\Delta Y_k|^2$ can be assumed nearly uncorrelated. Thus, they can be combined to obtain a more accurate estimate $|I_{\mathrm{comb},k}|^2$ of the impulsive interference power. It is proposed to combine both estimates linearly according to the variance of the signals $\hat{I}_k^{(\iota)}$ and D'_k given no impulsive interference occurred. Such a weighting is reasonable since the variances are a useful indicator for the quality of these signals and leads to

$$|I_{\mathrm{comb},k}|^2 = \frac{\mathrm{Var}\left(D'_k\right)\cdot|I_{\mathrm{iter},k}|^2+N_0\cdot|I_k|^2}{\mathrm{Var}\left(D'_k\right)+N_0}. \tag{48}$$

This estimate of the impulsive interference power can be directly incorporated in the FSBN algorithm from Section IV-A.

V. Complexity

Here, we examine the computational complexity of our proposed advanced BN algorithm. A common scheme for determining the computational complexity of algorithms is the big $\mathcal{O}$ notation. Conventional BN shows linear complexity; all N time domain samples are compared with BT. Consequently, the complexity is $\mathcal{O}(N)$. To determine the BT, a loop over a set of potential BTs is carried out. A typical range of BT is $T^{\mathrm{BN}} = [0, 10]$ with a step size of 0.1, leading to 100 runs. This number is for typical OFDM systems below or in the range of N; hence, we can approximate the additional complexity by $\mathcal{O}(N)$. Within the loop, the integrals from (7), (8), and (10) are realized as a sum. However, the calculation can be implemented as a cumulative sum, i.e., taking the values from the previous run and adding the current value. Consequently, the complexity of the loop stays $\mathcal{O}(N)$.The additional calculations for realistic channel conditions and frequency selective are performed outside this loop and also have a linear complexity of $\mathcal{O}(N)$. FSBN includes no loops or sums; consequently, the complexity is linear, i.e., $\mathcal{O}(N)$. It should be noted that FSBN requires an additional FFT that has complexity of $\mathcal{O}(N\log N)$, which can be realized in parallel, therefore not increasing complexity. Finally, the iterative receiver structure is considered. Since the number of iterations is a constant predefined number, it does not lead to an increase in complexity in terms of the $\mathcal{O}$ notation. The calculations within the iterations include no loops or sums but only basic operations for each subcarrier. Hence, the complexity stays $\mathcal{O}(N)$. In summary, the order of complexity for our proposed advanced BN stays the same as for the conventional BN and is $\mathcal{O}(N)$. Thus, it does not lead to a significant increase in complexity.

VI. Simulation Results

To evaluate the performance of the proposed algorithm, the transmission scenario from [3] is adopted. In this context, LDACS1 [28] as exemplarily chosen OFDM system is exposed to impulsive interference from the DME system.[3] LDACS1 operates at 994.5 MHz. The LDACS1 channel occupies $B = 625$ kHz bandwidth, resulting in a subcarrier spacing of $\Delta f \approx 9.8$ kHz, with $N = 64$ subcarriers. For channel coding, a concatenated scheme of a Reed–Solomon code with rate $r_{\mathrm{RS}} \approx 0.9$ and a convolutional code with rate $r_{\mathrm{CC}} = 1/2$ is used. The coded bits are quadrature phase shift keying (QPSK) modulated. This OFDM signal is interfered by Gaussian-shaped impulse pairs with short duration but high power, generated by DME stations. These stations are transmitting at a $\Delta f_c = \pm 0.5$ MHz frequency offset compared with the LDACS1 carrier frequency, however with a spectrum partially overlapping with the LDACS1 bandwidth. This leads to a frequency-selective impulsive interference, which mainly affects the edges of the LDACS1 bandwidth. The interference scenario from [3] comprises four DME stations, which are characterized in Table I. The starting times of the individual impulse pairs are modeled

[3]More detailed information about the two considered systems can be found in [3] and [28].

TABLE I
PARAMETERS OF INTERFERENCE SCENARIO

Station	Δf_c [MHz]	SIR [dB]	Impulse pair rate [1/s]
DME_1	-0.5	-18.7 + SNR [dB]	3600
DME_2	-0.5	-17.2 + SNR [dB]	3600
DME_3	-0.5	-2.9 + SNR [dB]	3600
DME_4	+0.5	-23.3 + SNR [dB]	3600

by independent Poisson processes. Such a process reflects the quasi-random occurrence of DME impulses. Consequently, there may occur OFDM symbols affected by impulse pairs form all four DME stations but also OFDM symbols that are affected by fewer DME stations or not affected by interference at all. This leads to a variety of different interference conditions with which our proposed algorithms have to cope. The signal-to-interference ratio (SIR) is defined as the ratio of P_s and the peak power P_i of DME impulses. The SNR is defined as P_s/N_0. Unlike the simulations, in real systems, an increasing SNR corresponds to an increasing OFDM signal power. This is taken into account when calculating the SIR by adding the SNR.

In addition to DME, we also consider a interference scenario with a constant PSD, named gated-Gaussian interference (GGI). This model has been considered for the investigations in [8] and [29]. Given the OFDM symbol index p, GGI is described by a gated-Gaussian process $i_{p,l}^{\mathrm{GGI}}$, which is the product of a gating process $v_{p,l}$ and a complex Gaussian process $g_{p,l}$, i.e.,

$$i_{p,l}^{\mathrm{GGI}} = v_{p,l} \cdot g_{p,l}. \tag{49}$$

For GGI, the term $g_{p,l}$ is characterized by a zero-mean complex Gaussian process with the variance σ_g^2 and the power $P_i^{\mathrm{GGI}} = 2\sigma_g^2$. The gating process samples $v_{p,l}$ are either one or zero. The occurrence of GGI is described by two variables. The first is the fraction of time β^{GGI} of an OFDM symbol during which GGI occurs. This fraction of time translates into N_{gate} affected samples in the considered OFDM symbol, which is calculated by

$$N_{\mathrm{gate}} = \lfloor \beta^{\mathrm{GGI}} N + 1/2 \rfloor. \tag{50}$$

Obviously, these samples occur as a contiguous block. As the interference bursts may occur very rarely, a repetition factor ζ is defined, determining that an interference burst occurs only in every ζth OFDM symbol. Based on these two parameters, the occurrence of GGI is mathematically described by

$$v_{p,l} = \begin{cases} 1, & \text{if } p \mod \zeta = 0 \ \wedge \\ & l = l^0, l^0+1, \ldots, l^0 + N_{\mathrm{gate}} - 1 \\ 0, & \text{else} \end{cases} \tag{51}$$

with l^0 being a randomly chosen number from $[0, 1, \ldots, N - N_{\mathrm{gate}}]$.

According to the intended operational frequency range of LDACS1, channel models for the lower part of the L-band from 960 to 1164 MHz have to be considered. For this frequency range, no generally accepted aeronautical channel model is available. When designing LDACS1, the very-high-frequency channel models from [30] have been adapted to the L-band [31]. These aeronautical L-band models have been derived mainly based on geometrical considerations [32] but take measurement data into account as well, e.g., to describe the Doppler pdf of scattered signal components [33]. Therefore, a good match with realistic transmission conditions is assumed. Consequently, the L-band models from [31] are adopted for our investigation. In particular, we apply the enroute (ENR) channel model and the terminal maneuvering area (TMA) channel model, basically corresponding to take-off and landing.

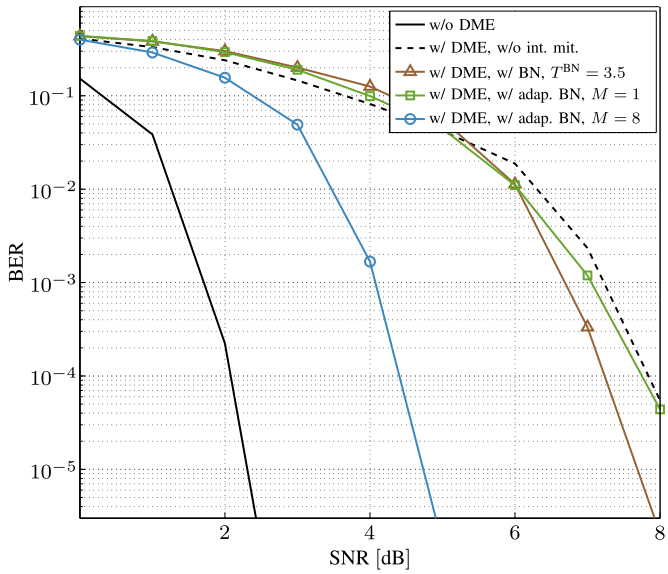

Fig. 3. Influence of BT calculation on coded BER of LDACS1 transmission versus SNR for AWGN channel and DME interference.

A. Adaptive BN

We start by assessing the influence of frequency-selective impulsive interference on the bit error rate (BER) performance for different ways of determining BT. We consider an LDACS1 transmission exposed to DME interference from Table I. In Fig. 3, BER is plotted versus SNR for different ways of determining BT. In particular, a fixed BT of $T^{\mathrm{BN}} = 3.5$ is compared with the adaptive BT calculation. The adaptive BT calculation is performed for $M = 1$ and $M = 8$ bins.[4] In addition, the performance for a transmission without interference, and a transmission with interference but without BN is shown. To separate distorting transmission channel effects from interference effects, an AWGN channel is applied.

For this simulation setup, BN with a fixed threshold of $T^{\mathrm{BN}} = 3.5$ only leads to moderate performance gain compared with a transmission without interference mitigation. When applying the adaptive BN with $M = 1$, no remarkable performance gain compared with a transmission without interference mitigation is achieved. Compared with the fixed BT, the performance is even slightly worse for high SNR due to the

[4]The selection of $M = 8$ has been derived empirically. For the OFDM system with different FFT sizes and/or different interference conditions, a different M may be appropriate. The optimal selection of M depends on many factors and is subject to further research. However, our investigations indicated that $M = \sqrt{(N)}$ is a good tradeoff.

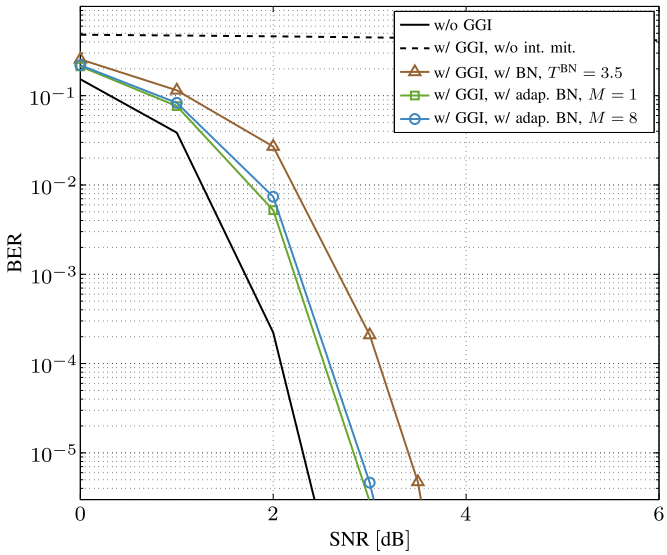

Fig. 4. Influence of BT calculation on coded BER of LDACS1 transmission versus SNR for AWGN channel and GGI with $\beta^{\mathrm{GGI}} = 0.1$, $\zeta = 2$, and SIR $= -15$ dB.

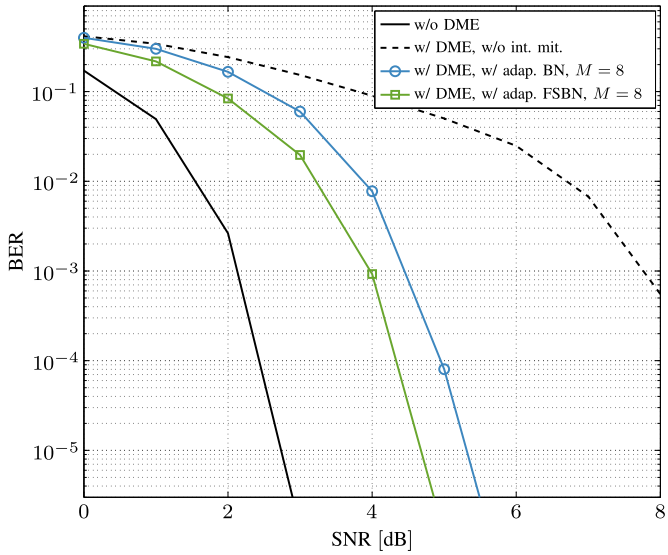

Fig. 5. Coded BER versus SNR of LDACS1 transmission for QPSK modulation, ENR channel, and DME interference; perfect knowledge of CTF. Comparison of BN and FSBN.

improper estimation of the interference power. However, when taking the spectral characteristics into account, segmenting the transmission bandwidth into $M = 8$ bins, and adjusting the threshold calculation, a huge performance gain is achieved. Compared with a transmission with a fixed BT of $T^{\mathrm{BN}} = 3.5$, the gain is ≈3 dB at BER $= 1 \times 10^{-5}$.

It is also of interest if the adjustment of the BT calculation to frequency-selective interference has an influence on the performance given interference with a constant PSD. Therefore, the earlier simulation setup is adopted, except for the interference model. The DME interference is replace by GGI, accounting for interference with a constant PSD. For GGI, $\beta^{\mathrm{GGI}} = 0.1$, $\zeta = 2$, and SIR $= -15$ dB are chosen. For this simulation setup, the BER is plotted versus the SNR in Fig. 4. Under such interference conditions, applying BN leads to a huge performance gain, independently of the BT calculation. Moreover, the adaptive BN with $M = 1$ leads to a gain of 0.5 dB at BER $= 1 \times 10^{-5}$ compared with the BN with a fixed BT of $T^{\mathrm{BN}} = 3.5$. When segmenting the transmission bandwidth into $M = 8$ bins and adjusting the threshold calculation, the performance loss compared with $M = 1$ is negligible small. Thus, particularly if no information regarding the type of impulsive interference is available, one should apply the spectral adjustment of the BT calculation by segmenting the bandwidth into bins. If the impulsive interference has a constant PSD, the performance nearly stays the same. However, if the impulsive interference shows frequency-selective behavior, remarkable gains can be achieved, as shown in Fig. 3.

B. Adaptive FSBN

To evaluate the performance of the FSBN algorithm, an LDACS1 transmission exposed to the DME interference scenario from Table I is selected. In addition, the ENR channel model described earlier is applied. The coded BER of an LDACS1 transmission is given in Fig. 5 versus the SNR, assuming perfect knowledge of the CTF. For the BT calculation, the OFDM transmission bandwidth is segmented into $M = 8$ bins. The performance of the FSBN is compared with the performance of the BN, also with $M = 8$ bins. As already presented in Fig. 3, the BN leads to a large improvement when segmenting the bandwidth into $M = 8$ bins. Compared with the BN, the proposed FSBN scheme achieves an additional gain of 0.6 dB at BER $= 1 \times 10^{-5}$. The remaining gap between the performance of the proposed scheme and the interference-free case is due to the reduction of OFDM signal power by BN and inaccuracies in estimating the SINR of R_k and Y_k. In addition, remaining ICI after the FSBN deteriorates the performance. This result indicates that the FSBN may work well even under realistic channel conditions, given the knowledge of the CTF. An imperfect knowledge of the CTF most likely degrades the performance of the FSBN algorithm. This issue is investigated in Section VI-C.

C. Iterative Receiver Structure

Next, we consider the potentials of iterative receiver structures. The coded BER of an LDACS1 transmission versus SNR is shown in Fig. 6. The TMA channel model and 2-D linear interpolation for CE are applied. The considered interference scenario is GGI with SIR $= -5$ dB, $\beta^{\mathrm{GGI}} = 0.1$, and $\zeta = 1$. For interference mitigation, the adaptive BN with $M = 8$ is considered. Since, for $\iota = 0$, no estimates of the channel coefficients are available for the calculation of the BT in the BN block, the BER tends toward an error floor. However, for $\iota > 0$, a significant iterative performance gain can be observed. A second iteration and a third iteration further improve the performance, confirming the beneficial influence of *a priori* information for BN. The gap between actually obtained and perfect *a priori* information is 1.8 dB at BER $= 1 \times 10^{-5}$. This gap is mainly due to the imperfect CE by 2-D linear interpolation.

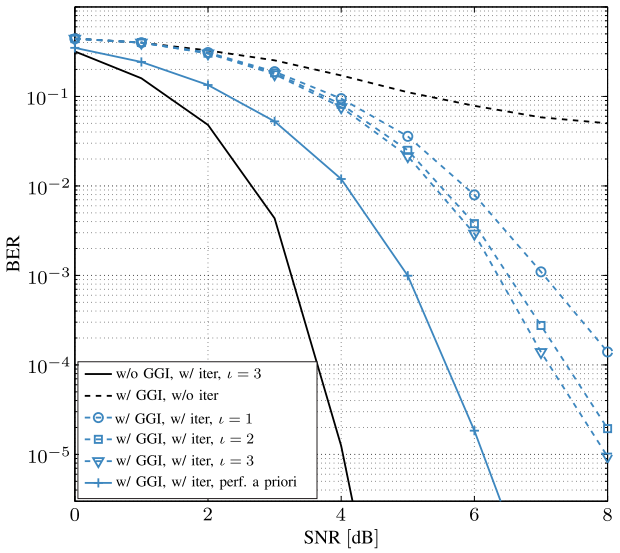

Fig. 6. Coded BER versus SNR of LDACS1 FL transmission. QPSK modulation, iterative receiver, TMA channel, GGI with $\beta^{\mathrm{GGI}} = 0.1$, $\zeta = 1$, SIR $= -5$ dB, CE by 2-D linear interpolation, and adaptive BN with $M = 8$.

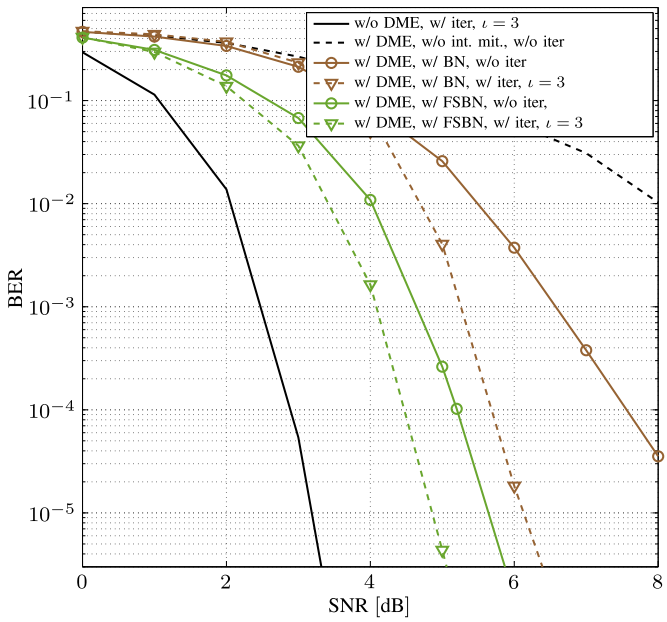

Fig. 7. Coded BER versus SNR of LDACS1 transmission; QPSK modulation, iterative receiver, ENR channel, DME interference, CE by 2-D linear interpolation, adaptive BN, and FSBN with $M = 8$.

Next, DME interference in combination with the ENR channel model is considered. For CE, a 2-D linear interpolation is adopted. For interference mitigation, the adaptive BN and the adaptive FSBN both with $M = 8$ are considered. The coded BER versus the SNR is shown in Fig. 7. These results illustrate the potentials of the proposed advanced BN. If no iterative loop is applied, we can observe a significant gain by BN and an additional gain of 1.2 dB at BER $= 1 \times 10^{-5}$ by FSBN. In the case of $\iota = 3$ iterations, both algorithms, i.e., adaptive BN and adaptive FSBN, benefit from the *a priori* information. For BN, the iterative gain is 2 dB at BER $= 1 \times 10^{-4}$; for FSBN, the iterative gain is 0.8 dB at BER $= 1 \times 10^{-5}$. The remaining gap between FSBN and the interference-free case is 1 dB at BER $= 1 \times 10^{-4}$. This gap is mainly due to ICI induced by BN. To further improve performance, the advanced BN could be combined with ICI cancelation schemes, such as in [3] and [4].

VII. Conclusion

In this paper, we elaborated on BN to mitigate impulsive interference in OFDM systems. BN is a popular mitigation scheme since it possesses a good tradeoff between low computational complexity and moderate performance gain. We characterized the drawbacks of BN in particular for OFDM systems and proposed advancements of conventional BN to compensate the various drawbacks. In particular, we introduced 1) an adaptive calculation of BT, 2) an FSBN, and 3) an iterative receiver structure including BN. Simulations showed that, depending on the characteristics of the impulsive interference, the different measures lead to considerable performance gain. Consequently, the different algorithms can be combined beneficially, leading to an OFDM receiver concept to cope with different kinds of impulsive interference. Finally, it should be emphasized that the proposed algorithms lead to a relatively low increase of computational complexity compared with conventional BN and require no information regarding interference characteristics. These two facts make our proposed advanced BN applicable to a wide range of OFDM systems.

References

[1] S. V. Zhidkov, "Performance analysis and optimization of OFDM receiver with blanking nonlinearity in impulsive noise environment," *IEEE Trans. Veh. Technol.*, vol. 55, no. 1, pp. 234–242, Jan. 2006.

[2] H. A. Suraweera, C. Chai, J. Shentu, and J. Armstrong, "Analysis of impulse noise mitigation techniques for digital television systems," in *Proc. 8th Int. OFDM Workshop*, Hamburg, Germany, 2003, pp. 172–176.

[3] S. Brandes, U. Epple, and M. Schnell, "Compensation of the impact of interference mitigation by pulse blanking in OFDM systems," in *Proc. IEEE Global Telecommun. Conf.*, Honululu, HI, USA, 2009, pp. 1–6.

[4] C.-H. Yih, "Iterative interference cancellation for OFDM signals with blanking nonlinearity in impulsive noise channels," *IEEE Signal Process. Lett.*, vol. 19, no. 3, pp. 147–150, Mar. 2012.

[5] S. V. Zhidkov, "Analysis and comparison of several simple impulsive noise mitigation schemes for OFDM receivers," *IEEE Trans. Commun.*, vol. 56, no. 1, pp. 5–9, Jan. 2008.

[6] K. M. Rabie and E. Alsusa, "Performance analysis of adaptive hybrid nonlinear preprocessors for impulsive noise mitigation over power-line channels," in *Proc. IEEE Int. Conf. Commun.*, London, U.K., 2015, pp. 728–733.

[7] S. Zhidkov, "Impulsive noise suppression in OFDM-based communication systems," *IEEE Trans. Consum. Electron.*, vol. 49, no. 4, pp. 944–948, Nov. 2003.

[8] J. Armstrong and H. A. Suraweera, "Decision directed impulse noise mitigation for OFDM in frequency selective fading channels," in *Proc. IEEE Global Telecommun. Conf.*, Dallas, TX, USA, 2004, pp. 3536–3540.

[9] G. Caire, T. Al-Naffouri, and A. Narayanan, "Impulse noise cancellation in OFDM: An application of compressed sensing," in *Proc. IEEE Int. Symp. Inf. Theory*, Toronto, ON, Canada, 2008, pp. 1293–1297.

[10] J. Lin, M. Nassar, and B. Evans, "Non-parametric impulsive noise mitigation in OFDM systems using sparse bayesian learning," in *Proc. IEEE Global Telecommun. Conf.*, Houston, TX, USA, 2011, pp. 1–5.

[11] S. Liu, F. Yang, W. Ding, and J. Song, "Double kill: Compressive sensing based narrowband interference and impulsive noise mitigation for vehicular communications," *IEEE Trans. Veh. Technol.*, vol. 65, no. 7, pp. 5099–5109, Jul. 2016.

[12] J. Häring and A. J. H. Vinck, "Iterative decoding of codes over complex number for impulsive noise channels," *IEEE Trans. Inf. Theory*, vol. 49, no. 5, pp. 1251–1260, May 2003.

[13] F. Abdelkefi, P. Duhamel, and F. Alberge, "Impulsive noise cancellation in multicarrier transmission," *IEEE Trans. Commun.*, vol. 53, no. 1, pp. 94–106, Jan. 2005.
[14] K. A. Saaifan and W. Henkel, "Lattice signal sets to combat pulsed interference from aeronautical signals," in *Proc. IEEE Int. Conf. Commun.*, Kyoto, Japan, 2011, pp. 1–5.
[15] U. Epple and M. Schnell, "Adaptive threshold optimization for a blanking nonlinearity in OFDM receivers," in *Proc. IEEE Global Telecommun. Conf.*, Anaheim, CA, USA, 2012, pp. 3661–3666.
[16] U. Epple, D. Shutin, and M. Schnell, "Mitigation of impulsive frequency-selective interference in OFDM based systems," *IEEE Wireless Commun. Lett.*, vol. 1, no. 5, pp. 484–487, Oct. 2012.
[17] F. Sarabchi and C. Nerguizian, "Impulsive noise mitigation for OFDM-based systems using enhanced blanking nonlinearity," in *Proc. IEEE 25th Annu. Int. Symp. Pers., Indoor, Mobile Radio Commun.*, Washington, DC, USA, 2014, pp. 841–845.
[18] D. Darsena, G. Gelli, F. Melito, and F. Verde, "ICI-free equalization in OFDM systems with blanking preprocessing at the receiver for impulsive noise mitigation," *IEEE Signal Process. Lett.*, vol. 22, no. 9, pp. 1321–1325, Sep. 2015.
[19] F. Sanzi, S. Jelting, and J. Speidel, "A comparative study of iterative channel estimators for mobile OFDM systems," *IEEE Trans. Wireless Commun.*, vol. 2, no. 5, pp. 849–859, Sep. 2003.
[20] S. Sand, C. Mensing, and A. Dammann, "Transfer chart analysis of iterative OFDM receivers with data aided channel estimation," in *Proc. 3rd Cost 289 Workshop*, Aveiro, Portugal, Jul. 2006, pp. 1–5.
[21] S. Ten Brink, J. Speidel, and R.-H. Han, "Iterative demapping for QPSK modulation," *Electron. Lett*, vol. 34, no. 15, pp. 1459–1460, Jul. 1998.
[22] H. Zhang and X.-G. Xia, "Iterative decoding and demodulation for single-antenna vector OFDM systems," *IEEE Trans. Veh. Technol.*, vol. 55, no. 4, pp. 1447–1454, Jul. 2006.
[23] U. Epple, K. Shibli, and M. Schnell, "Investigation of blanking nonlinearity in OFDM systems," in *Proc. IEEE Int. Conf. Commun.*, Kyoto, Japan, 2011, pp. 1–5.
[24] D. Pauluzzi and C. Beaulieu, "A comparison of SNR estimation techniques for the AWGN channel," *IEEE Trans. Commun.*, vol. 48, no. 10, pp. 1681–1691, Oct. 2000.
[25] A. Wiesel, J. Goldberg, and H. Messer-Yaron, "SNR estimation in time-varying fading channels," *IEEE Trans. Commun.*, vol. 54, no. 5, pp. 841–848, May 2006.
[26] H. Suraweera and J. Armstrong, "Noise bucket effect for impulse noise in OFDM," *Electron. Lett.*, vol. 40, no. 18, pp. 1156–1157, Sep. 2004.
[27] S. M. Kay, *Fundamentals Of Statistical Processing, Volume 2: Detection Theory*. Upper Saddle River, NJ, USA: Pearson, 2009.
[28] Updated LDACS1 System Specification, 2011. [Online]. Available: www.sesarju.eu, SESAR JU Std.
[29] J. Lago-Fernandez and J. Salter, "Modelling impulsive interference in DVB-T: Statistical analysis, test waveforms and receiver performance," BBC Res. Develop., London, U.K., Tech. Rep., 2004.
[30] "Software implementation of broadband vhf radio channel models," B-VHF consortium, Luxembourg, B-VHF project, Tech. Rep. D-17, 2006.
[31] "Report d5, expected B-AMC system performance," EUROCONTROL, Brussels, Belgium, B-AMC consortium Tech. Rep., 2007, p. 1.
[32] E. Haas, "Aeronautical channel modeling," *IEEE Trans. Veh. Technol.*, vol. 51, no. 2, pp. 254–264, Mar. 2002.
[33] A. Neul, J. Hagenauer, W. Papke, F. Dolainsky, and F. Edbauer, "Propagation measurements for the aeronautical satellite channel," in *Proc. IEEE Veh. Technol. Conf.*, Tampa, FL, USA, 1987, pp. 90–97.

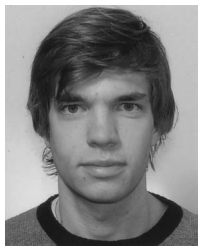

Ulrich Epple received the Dipl.-Ing. (M.Sc.) degree in electrical engineering and the Dr.-Ing. (Ph.D.) degree for his work on impulsive interference mitigation in orthogonal-frequency-division-multiplexing-based systems from the University of Ulm, Ulm, Germany, in 2008 and 2014, respectively.

From 2008 to 2015, he was a Scientific Researcher with the Institute of Communications and Navigation, German Aerospace Center (DLR), Oberpfaffenhofen, Germany. He has been involved mainly in the development of future digital data links for aeronautical communications. This covers the development of interference mitigation schemes, as well as synchronization, channel estimation, and channel coding aspects.

Michael Schnell (M'96–SM'04) received the Dipl.-Ing. (M.Sc.) and Dr.-Ing. (Ph.D.) degrees in electrical engineering in 1987 and 1997, respectively.

Since 1990, he has been a Scientific Researcher with the Institute of Communications and Navigation, German Aerospace Center (DLR), Oberpfaffenhofen, Germany, where he is currently the Group Leader and the Project Manager of the Aeronautical Communications Group. He is a Lecturer on multicarrier communications and acts as a Selected Advisor for the German air navigation service provider (DFS GmbH).